Revised Version 10.3.2009

# Substituent Effects on $^{61}$Ni NMR Chemical Shifts.[‡]

**Michael Bühl,[a]\*, Dietmund Peters[b], Rainer Herges[b]**

[a] School of Chemistry, North Haugh, University of St. Andrews, St. Andrews, Fife KY16 9ST, UK, Fax: +(44)(0)1334 463808, E-mail: buehl@st-andrews.ac.uk; previous address: Max-Planck-Institut für Kohlenforschung, Kaiser-Wilhelm-Platz 1, D-45470 Mülheim an der Ruhr, Germany.

[b] Otto-Diels-Institut für Organische Chemie, Universität Kiel, rherges@oc.uni-kiel.de.

**Abstract**

$^{61}$Ni chemical shifts of Ni(all-*trans*-cdt)L (cdt = cyclododecatriene, L = none, CO, PMe$_3$), Ni(CO)$_4$, Ni(C$_2$H$_4$)$_2$(PMe$_3$), Ni(cod)$_2$ (cod = cyclooctadiene), and Ni(PX$_3$)$_4$ (X = Me, F, Cl) are computed at the GIAO (gauge-including atomic orbitals)-, BPW91-, B3LYP-, and BHandHLYP levels, using BP86-optimised geometries and an indirect referencing scheme. For this set of compounds, substituent effects on δ($^{61}$Ni) are better described with hybrid functionals than with the pure BPW91 functional. On going from Ni(all-*trans*-cdt) to Ni(all-*cis*-cdt) the computations predict a substantial shielding by nearly 700 ppm for the $^{61}$Ni nucleus, as well as a sharp increase of the electric field gradient at its position. The latter result is indicated to afford an undetectably broad $^{61}$Ni NMR line for the all-*cis*-cdt complex, rationalizing the apparent failure to record the NMR spectrum experimentally.

**Key words**: NMR, $^{61}$Ni, Density functional calculations, Chemical shift computations, Electric field gradient

---

[‡] Dedicated to Prof. Walter Thiel on the occasion of his 60th birthday.

# 1 Introduction

Cyclododecatriene-nickel(0), one form of "naked nickel", is a textbook example of a low-valent transition metal complex that is useful as a convenient metal source for synthesis and catalysis.[1,2] The all-trans form (**1**) was the first isolated nickel(0)-olefin complex and has long been characterised thoroughly.[3] The structure of the thermodynamically more stable, but also more reactive, all-cis isomer (**2**) has been solved recently.[4] In both complexes, the three double bonds are coordinated in a trigonal planar fashion about the central metal. The simplest tris(olefin)nickel complex, tris(ethylene)nickel(0) (**3**) can be prepared in crystalline form,[5] but is highly labile and too reactive for detailed spectroscopic observation in solution. This complex has recently attracted interest from theory, as computed magnetic response parameters have led to the suggestion that the $D_{3h}$-symmetric minimum (**3a**) with the three $\pi$-bonds all in the same plane could allow cyclic delocalisation of these $\pi$-electrons, thereby sustaining a diatropic ring current characteristic of Hückel-aromatic compounds.[6] This conclusion was based on plots of the induced current density and, apparently, supported by the computed $^{61}$Ni chemical shifts of **3a** and the perpendicular variant **3b**, where any such delocalisation would be shut off: The metal nucleus in **3a** was predicted to be much more shielded, by more than 1800 ppm, than that in **3b**, in line with the expectation that a magnetic probe placed at the centre of a diatropic ring current should experience a substantial upfield shift.[7]

<Scheme 1>

Quantitatively, this huge difference in $\delta(^{61}$Ni) values is far too large to be ascribed solely to such benzene-like ring currents, because the latter are independent of the probe nucleus, and would be the same in ppm for the metal as for any other lighter nucleus such as $^1$H.[8] Typical effects for protons located in the shielding cones of aromatic compounds amount to but a few ppm,[7b] and the largest upfield shift due to ring currents, $\delta(^3$He) of endohedral He complexes of "superaromatic" fullerene anions do not exceed -50 ppm.[9] Qualitatively, however, the use of $^{61}$Ni chemical shifts as a probe into the electronic structure of Ni complexes is of interest, taking advantage of the broad chemical shift range and sensitivity towards substituent effects that is typical for transition-metal NMR.[10] In the heyday of nickel chemistry, $^{61}$Ni NMR has been employed as means of spectroscopic characterisation for a number of complexes,[11,12] but the problems associated with the large quadrupole moment of this nucleus have hindered widespread analytical applications.

We have become interested in using this technique to probe the electronic structures of **1** and **2** and to investigate to which extent they reflect those of the parent ethylene complexes **3b** and **3a** (noting that the olefins are essentially in-plane in both **2** and **3a**, strongly twisted in **1**, and exactly perpendicular in the elusive **3b**). Preliminary CSGT-B3LYP/6-31+G(d) computations indeed indicated a large difference between $\delta(^{61}Ni)$ of **1** and **2** (ca. 700 ppm).[13] However, the sensitivity of DFT-computed transition-metal chemical shifts toward the exchange-correlation functional is highly variable,[14] and can, depending on the nucleus under scrutiny, range from fairly feeble to downright dramatic.[15] This situation calls for a systematic test of computation of $^{61}Ni$ chemical shifts in order to gauge the accuracy of the DFT results. Simultaneously, an independent experimental confirmation of the DFT predictions for **2** seemed desirable. The present paper summarises our efforts toward these goals. As it turns out, the reliability of theoretical $^{61}Ni$ NMR chemical shifts can be improved by adopting an indirect referencing procedure, and DFT results can be used to rationalise the apparent failure to record the $^{61}Ni$ NMR spectrum of **2**.

## 2 Experimental and Computational Details

### 2.1 DFT Computations

Methods and basis sets correspond to those used in the previous studies of first-row transition-metal complexes:[15] Geometries have been fully optimised in the given symmetry at the BP86/AE1 level, i.e. employing the exchange and correlation functionals of Becke[16] and Perdew,[17] respectively, together with a fine integration grid (75 radial shells with 302 angular points per shell), the all-electron Wachters basis augmented with 2 diffuse d and one diffuse p sets (contraction scheme 62111111/3311111/3111), and standard 6-31G(d) basis set[18] for all other elements (except for the C atoms of the phosphine *t*Bu and *i*Pr groups, for which 6-31G basis was used). All structures have been characterised as minima by the absence of imaginary harmonic vibrational frequencies.

Magnetic shieldings $\sigma$ have been evaluated for the BP86 optimised geometries using a popular implementation[19] of the GIAO (gauge-including atomic orbitals)-DFT method involving the functional combinations according to Becke[3] and Perdew and Wang[20] (denoted BPW91), Becke (hybrid)[21] and Lee, Yang, and Parr[22] (denoted B3LYP), or Becke (half-and-half, using 50% of Hartree-Fock exchange) and Lee, Yang, and Parr (denoted BHandHLYP).[23] These computations employed basis II', i.e. the same augmented Wachters basis on Ni, and the recommended IGLO-basis II[24] on all other atoms except hydrogen and the C atoms of the phosphine *t*Bu and *i*Pr groups, where a double-zeta (DZ) basis was used. In order to convert $\sigma$ values into relative chemical shifts $\delta$, the shielding constants of the standard have been evaluated as the y-intercept of linear regressions

of computed $\sigma$ vs. experimental $\delta$ values at each level. The resulting $\sigma$(standard) values are -1510, -1657, and -1929 ppm at the GIAO-BPW91, -B3LYP, and -BHandHLYP levels, respectively. Preliminary NMR computations have been performed at the CSGT-(continuous set of gauge transformations)-B3LYP/6-31G(d) level (for geometries optimised at the same DFT level[25]), using $Ni(CO)_4$ directly as reference, with a $\sigma$(standard) value of -2212 ppm.

EFGs have been computed at the B3LYP/II' level employing the BP86 geometries. The largest component of the EFG tensor, $q_{zz}$, is given (reported in atomic units, 1 au = $9.717365 \cdot 10^{21}$ $Vm^{-2}$ for conversion into *eq* values). These static quantum-chemical computations employed the Gaussian 98 suite of programs.[26]

*2.2 Experimental*

**Ni-*all-trans*-cyclododecatriene 1** was synthesised from freshly sublimed Ni-acetylacetonate, *all-trans*-cyclododecatriene and diethylaluminumethoxide (as the reducing agent) in THF according to a procedure of Wilke et al.[27] Complex **1** was purified by vacuum sublimation ($<10^{-5}$ Torr). The metallic glossy, deep red crystals are indefinitely stable in a rigorously oxygen-free atmosphere. Solutions in benzene and THF, even prepared under careful exclusion of oxygen, decompose within a few days forming a nickel mirror. To prevent the formation of paramagnetic nickel, and to allow the NMR investigation, we added 0.5 equivalents of di-*tert*-butylisopropylphosphine. Solutions containing this bulky phosphine ligand are stable for several days without decomposition.[28] $^{61}$Ni spectra were recorded on a Bruker AV 400 spectrometer. **$^1$H-NMR** (200.1 MHz, [$D_6$]benzene, 300 K, benzene): $\delta$ = 4.28 ($m_c$, 6H; CH), 2.39 ($m_c$, 6H; $H_{eq}$), 1.99 ($m_c$, 6H; $H_{ax}$), 1.30 ((dd, $^3J$(P,H) = 10.5 Hz, $^3J$(H,H) = 7.4 Hz, 6H; P–CH(CH$_3$)$_2$ ), 1.18 (d, $^3J$(H,P) = 10.5 Hz, 18H; P–C(CH$_3$)$_3$ ); **$^{13}$C-NMR** (50.3 MHz, [$D_6$]benzene, 300 K, benzene, DEPT 135): $\delta$ = 107.2 (t), 41.8 (s; CH$_2$), 33.5 (q, d, $^1J$(C,P) = 27.6 Hz; P–C(CH$_3$)$_3$), 31.7 (p, d, $^2J$(C,P) = 13.9 Hz; P–C(CH$^3$)$^3$), 25.5 (t, d, $^1J$(C,P) = 28.4 Hz; P–CH(CH$_3$)$_2$), 24.0 (p, d, $^2J$(C,P) = 13.7 Hz; P–CH(CH$_3$)$_2$; **$^{31}$P-NMR** (81.0 MHz, [$D_6$]benzene, 300 K, H$_3$PO$_4$ (external)): $\delta$ = 46.8 **$^{61}$Ni-NMR** (35.8 MHz, [$D_6$]benzene, 300 K, Ni(CO)$_4$ (substitutive), c = 0.17 mol L$^{-1}$): $\delta$ = 75 (s;$v_{1/2}$ = 3.9 kHz) (*fid shift*); the spectral data of this phosphine-stabilised solution are consistent with previous reports for pure **1**.[29]

**Ni-*all-cis*-cyclododecatriene 2** was prepared from the *all-trans* complex **1** and *all-cis*-cyclododecatriene by ligand exchange according to Wilke et al.[30] The complex was purified by vacuum sublimation ($<10^{-5}$ Torr) and was obtained as yellow needles (which, however, decomposed

and turned black in our hands when exposed to an inert atmosphere in a glovebox). The *all-cis* complex **2** is even more oxygen sensitive than its *all-trans* isomer. To obtain stable solutions expected to contain **2** for NMR investigations, the ligand exchange reaction was performed in an NMR tube by adding *all-cis*-cyclododecatriene to a phosphine stabilised solution of *all-trans*-cyclododecatriene **1** under argon. **$^1$H-NMR** (500.1 MHz, [D$_8$]THF, 300 K, THF): δ = 4.97 (s, 6H; CH *all-trans* **1**), 4.83–4.76 (m, 6H; CH *all-cis* **2**), 2.48–2.32 (m, 12H; CH$_2$ *all-cis* **2**), 2.01 (s, 16H; CH$_2$ *all-trans* **1**), 1.90 (sep, $^3J$(H,H) = 7.4 Hz, 1H; P–C$\underline{H}$(CH$_3$)$_2$), 1.34 (dd, $^3J$(P,H) = 9.8 Hz, $^3J$(H,H) = 8.2 Hz, 6H; P–CH(C$\underline{H}_3$)$_2$), 1.20 d, $^3J$(H,P) = 10.0 Hz, 18H; P–C(CH$_3$)$_3$); **$^{13}$C-NMR** (125.8 MHz, [D$_8$] THF, 300 K, THF, DEPT 135): δ = 132.3 (t; CH *all-trans* **1**), 89.8 (t; CH *all-cis* **2**), 33.3 (s; CH$_2$ *all-trans* **1**), 29.5 (s; CH$_2$ *all-cis* **2**); **$^{31}$P-NMR** (202.5 MHz, [D$_8$]THF, 300 K, H$_3$PO$_4$ (external)): δ = 47.7 (phosphine). **$^{61}$Ni-NMR** (35.8 MHz, [D$_6$]benzene, 300 K, Ni(CO)$_4$ (substitutive), c = 0.17 mol · L$^{-1}$): δ = 22 (*fid shift*) respectively 17 (difference) (s; ν$_{1/2}$ = 8.9 kHz). Again the $^1$H and $^{13}$C data of this phosphine-stabilised solution (which contained traces of **1**) are consistent with previous reports for **2**.[29b,c]

**Tetrakis(trimethylphosphine)nickel(0) 10.** Our attempts to prepare **10**[31] by an alternative route from Ni-*all-trans*-cyclododecatriene **1** and trimethylphosphine resulted in a mixture of the rather stable and known adduct **1**·P(CH$_3$)$_3$[29] and Ni(PMe$_3$)$_4$, as both components were identified by their NMR data. Nevertheless we have been able to detect the typical $^{61}$Ni NMR reference of Ni(PMe$_3$)$_4$: **$^{61}$Ni-NMR** (35.8 MHz, [D$_6$]benzene, 300 K, Ni(CO)$_4$ (substitutive), c = 0.15 mol · L$^{-1}$): δ = 35 (q, $^1J$(P,Ni) = 287 Hz; ν$_{1/2}$ = 20 Hz).

<Scheme 2> <Table 1>

## 3 Results and Discussion

This section is organised as follows: First, a systematic assessment of DFT methods for the computation of $^{61}$Ni chemical shifts is presented, calling special attention to the use of generalised gradient approximation (GGA) versus hybrid functionals. Next, our experimental efforts to record the $^{61}$Ni NMR spectrum of **2** are summarised, followed by a brief discussion of phosphine complexation and electric field gradients at the metal centre.

*3.1 Validation of the DFT methods*

In addition to complex **1**, the test set of this study comprises the compounds **4** - **11** depicted in Scheme 2, which cover essentially the whole known range of $^{61}$Ni chemical shifts. Salient BP86-optimised geometrical parameters for **1** -**11** are collected in Table 1, together with experimental data from gas-phase electron diffraction[32,33] or X-ray crystallography,[4,3,34,35,36] where available. In general, the theoretical data compare favorably to the experimental values, with bond lengths typically agreeing to a few pm. Optimised bond distances tend to be overestimated, as is frequently observed with DFT results for transition metal complexes.[37] The agreement with experiment could probably be slightly improved by using a recent hybrid-meta-functional instead of BP86 in the optimisations.[38] For consistency with previous studies on first-row transition metal NMR parameters, however, we continue to use BP86 geometries.

The latter were subsequently employed as inputs for NMR chemical shift computations at the GIAO-BPW91 and GIAO-B3LYP levels. These levels were chosen for compatibility with our previous work on transition-metal chemical shifts and should be representative for other GGA and hybrid functionals, respectively. For $^{53}$Cr, for instance, magnetic shieldings have been found to be very similar at GIAO-BPW91 and GIAO-BP86 GGA levels,[39] and for $\delta(^{55}Mn)$ B3LYP and mPW1PW91 hybrid functionals have performed quite similar.[15d] When the $^{61}$Ni chemical shifts were referenced directly to $Ni(CO)_4$ (**4**), the experimental standard, and plotted vs. the experimental data, the resulting slopes of the linear regression lines were ca. 0.8 and 0.9 at the BPW91 and B3LYP levels, respectively. As in all cases studied before, inclusion of Hartree-Fock (HF) exchange increases the paramagnetic contributions to the shielding constants proportionally, thus increasing the $\delta_{calc}/\delta_{exp}$ slope. The preliminary results for $^{61}$Ni chemical shifts suggested that raising the amount of HF exchange in the functional (which is 20% in B3LYP) could bring this slope even closer to the ideal value, unity. This expectation was borne out by subsequent GIAO-BHandHLYP computations (with 50% HF exchange), which afforded a near-ideal slope. In the "raw" (i.e. directly referenced) hybrid DFT data, however, systematic offsets with respect to experiment became apparent, as all computed $\delta$ values were too strongly shielded by ca. 300 and 500 ppm at B3LYP and BHandH levels, respectively. Apparently, HF exchange increases the paramagnetic contributions in **4** far too much compared to the other complexes.

In view of this problem with the standard, it was decided to adopt an alternative referencing scheme. As in cases where the actual standard is difficult or impossible to compute (e.g. when it is highly charged[15c] or when just a standard frequency is used[15a]), the reference shielding for $^{61}$Ni NMR was obtained from a linear regression of computed $\sigma$ vs. experimental $\delta$ values (excluding **4** from this

analysis). The resulting σ(standard) values are given in section 2.1, and the corresponding chemical shifts are summarised in Table 2 and plotted versus the experimental data in Figure 1.

<Table 2> <Figure 1>

The various density functionals are best assessed in terms of mean absolute deviations (MAD) from experiment and by the slopes of the corresponding linear regression lines (last two entries in Table 2). By these criteria, the BPW91 functional is clearly inferior to the two hybrid variants, as it affords the smallest slope (0.85) and the largest MAD (more than 100 ppm). The performance of B3LYP and BHandHLYP is quite similar, the former somewhat underestimating the slope (0.93), the latter slightly overestimating it (1.04), and both have comparable MADs. Because the mean error of B3LYP (65 ppm) is slightly smaller than that of BHandHLYP (73 ppm), and for consistency with the majority of transition metal nuclei studied so far, we recommend the B3LYP functional for the computation of $^{61}$Ni chemical shifts. This nucleus thus fits nicely into the pattern established so far, according to which it is the centre of each transition row where GGAs perform best (e.g. for $^{53}$Cr in the 3d series),[39] and the later metals where HF exchange is beneficial (e.g. for $^{55}$Mn and $^{57}$Fe).[15a,d]

The MAD of 65 ppm achieved with B3LYP corresponds to 3.5% of the total chemical shift range covered, a rather respectable accuracy for present-day DFT. The improvement over the GGA, however, comes at the expense of the description of the standard, **4**, which deteriorates with the amount of HF exchange included (see the data point at $\delta_{expt}$ =0 in Figure 1). In order to probe if rovibrational corrections could affect this result, we computed zero-point contributions to the magnetic shieldings of **4** and **9** (the latter of which is a representative phosphine complex at the shielded end of the $^{61}$Ni chemical shift scale). Inclusion of anharmonicity corrections to the geometrical parameters via an established perturbational scheme[40] decreases the σ values of the metal in **4** and **9** by -54 and -26 ppm, respectively (affording so-called "effective" $\sigma_{eff}$ values). These are relatively minor changes, suggesting that evaluating these corrections to the whole test set (i.e. going beyond the static equilibrium shifts discussed so far) would alter the results only marginally.

To summarise this part, the combination of BP86-optimised geometries, B3LYP-derived magnetic shielding constants, and an indirect referencing scheme has emerged as practical tool to compute $^{61}$Ni chemical shifts. With this protocol the literature value of **1**, $\delta(^{61}Ni)_{exp}$ = 206 ppm, is reproduced within a few ppm (see Table 2), and the $^{61}$Ni chemical shift of **2** is predicted to be shifted upfield by

669 ppm, at $\delta(^{61}Ni)_{calc} = -468$ ppm. We now turn to our attempts to verify this prediction experimentally.

### 3.2 $^{61}Ni$ NMR studies

The recording of $^{61}Ni$ NMR spectra is extremely challenging for several reasons. The natural abundance of the magnetically active isotope is low (1.19%), the receptivity is only about 1/5 of $^{13}C$ and because of the large quadrupole moment of $^{61}Ni$ unsymmetrical complexes exhibit extremely broad signals (up to several KHz). Moreover, the low resonance frequency of 8.936050 MHz [$\nu(^1H)=100$ MHz] leads to technical problems while recording the spectra. The samples of **1** and **2** in [$D_6$]benzene had to be stabilised by adding 0.5 equivalents of di-*tert*-butylisopropylphosphine to prevent the formation of metallic nickel.

$^{61}Ni$ chemical shifts are solvent dependent. Tetrakis(trimethylphosphine)nickel(0) **10** which is frequently used as a reference in $^{61}Ni$ NMR (instead of the toxic Ni(CO)$_4$) exhibits a $^{61}Ni$ NMR signal (with respect to Ni(CO)$_4$) at 40 ppm in [$D_8$]THF[12] and at 15.2 ppm in [$D_8$]toluene.[11b] We observed the characteristic quintet of **10** in [$D_6$]benzene at 35 ppm ($^1J$(P, Ni)=287 Hz, $\nu_{1/2}$=20Hz). The less symmetric Ni-*all-trans*-cyclododecatriene **1** resonates at 75 ppm with a much broader signal ($\nu_{1/2}$ =3.9 KHz). The seemingly large deviation from the value determined by Benn et al. (206 ppm in [$D_8$]THF) is probably due to solvent effects. For the sample expected to contain Ni-*all-cis*-cyclododecatriene **2** a very broad signal ($\nu_{1/2}$=8.9KHz) at 22 ppm was observed which is about 50 ppm upfield as compared to the *all-trans* isomer. While the broadening and the upfield shift are expected for the *all-cis*-isomer **2** the absolute value of the shift deviates considerably from the calculated value.

### 3.3 Phosphine Addition and Electric Field Gradients

A possible explanation of the apparent discrepancy between predicted and observed $^{61}Ni$ chemical shifts of **2** could be that under the experimental conditions a different species is present. In particular, the bulky phosphine added to improve the stability of the solution might interact more strongly with **2** than with **1**. That the phosphine does not coordinate to **1**, at least not to any significant extent, is obvious from the absence of any noticeable downfield shift of the $^{61}Ni$ resonance form the literature value (a strong such shift is to be expected upon phosphine coordination, cf. the data in Table 2 for **1** and its PMe$_3$ adduct, **8**). In **2**, however, where the metal is somewhat more exposed to one side, steric hindrance toward phosphine coordination might be less pronounced than in **1**, and population of adducts of the type Ni(c,c,c-cdt)[P(*t*Bu)$_2$(*i*Pr)], e.g. in an

equilibrium, might become noticeable.[41] Because the observed $^{31}$P NMR signal of the phosphine is unchanged in the presence of Ni(cdt) complexes, such a scenario would require either a zero complexation shift of the $^{31}$P resonance, or a very small amount of such phosphine complexes and, concomitantly, a huge difference in $\delta(^{61}Ni)$ between these phosphine complexes and free **2**. In order to explore these possibilities, we have optimised a few representative adducts of this kind and computed their $^{31}$P and $^{61}$Ni chemical shifts. We did not perform full conformational analyses (e.g. concerning the possible orientations of the *i*Pr groups[42]), trusting that, in particular, the $^{61}$Ni NMR parameters will not depend drastically on such structural details more than two bonds away from the metal.
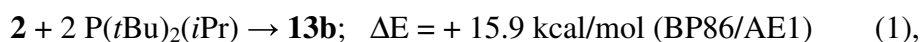
<Figure 2>

For the all-*trans* species **1**, a four-coordinate minimum with intact $\eta^6$-bonding of the olefin can be located (**12**, Figure 2). At the uncorrected BP86/AE1 level, i.e. without corrections for basis-set superposition error, zero-point energies and entropies (which all would serve to disfavor formation of the phosphine complex), the phosphine in **12** is computed to be unbound by 7.9 kcal/mol with respect to free **1** and P(*t*Bu)$_2$(*i*Pr). At $\delta$=1233 ppm, the Ni atom in **12** is predicted to be even more deshielded than that in the PMe$_3$ parent **8**, underscoring that **12** is not formed in the NMR experiments.

As expected,[4] no such four-coordinate minimum can be located for the corresponding all-*cis* form, where the phosphine spontaneously dissociates during the optimisation. The most stable isomer with reduced hapticity of the olefin that could be located is Ni($\eta^4$-c,c,c-cdt){P(*t*Bu)$_2$(*i*Pr)} (**13a**, Figure 2), with a raw phosphine binding energy of +3.5 kcal/mol at BP86/AE1 (+0.8 kcal/mol at B3LYP/II'), relative to free **2** and P(*t*Bu)$_2$(*i*Pr). For **13a**, $\delta(^{61}Ni)$ = -55 ppm is obtained, noticeably shielded from that in **1** with $\delta(^{61}Ni) \approx 200$ ppm (Table 2). The rather large difference between **13a** and the formally analogous bis(olefin)phosphine complex **5** ($\delta \approx$ -900 ppm) is noteworthy. Among other substituent effects, the different degree of twisting of the olefin moieties may be responsible for this result: whereas the olefinic C atoms are essentially within the trigonal coordination plane in **5**, they are significantly twisted in **13a** (cf. the P-Ni-C-C dihedral angles of ca. 180 ° and 145° in **5** and **13a**, respectively), much like the difference between **1** and **2** discussed above. Population of **13a** in rapid equilibrium with **2** could shift the $\delta(^{61}Ni)$ value of the latter (−468 ppm) to more positive values. However, in order to approach the observed $^{61}$Ni resonance initially ascribed to **2** (ca. +20 ppm), such an equilibrium would have to be shifted far to the side of **13a**. This possibility

can be excluded because in that case, the complexation shift of the $^{31}$P resonance would be noticeable: the $^{31}$P nucleus in **13a** is predicted to be deshielded by 25 ppm relative to that in the free phosphine, a substantial amount that would not go unnoticed.

If, upon substitution of more coordinated olefins by phosphines, the Ni nucleus would become more deshielded, a smaller fraction of such complexes in an equilibrium with **2** could account for the observed $^{61}$Ni resonance. Indeed, $\delta = 415$ ppm is predicted for a representative Ni($\eta^2$-c,c,c-cdt){P($t$Bu)$_2$($i$Pr)}$_2$ complex (**13b**, Figure 2), implying that more than 50% of **13b** would be necessary in equilibrium with **2** to reproduce the observed chemical shift. Such a situation is highly unlikely, however, given the pronounced endothermicity of the formation reaction according to

$$2 + 2\ P(t\text{Bu})_2(i\text{Pr}) \rightarrow \textbf{13b};\quad \Delta E = +\ 15.9\ \text{kcal/mol (BP86/AE1)} \qquad (1),$$

and the expected substantial entropic penalty.[43] The latter would favor olefin dissociation in **13b** affording free c,c,c-cdt and Ni{P($t$Bu)$_2$($i$Pr)}$_2$, a process that is already exothermic by 4.4 kcal/mol (BP86/AE1 level). The latter bis(phosphine) nickel complex[44] has a computed $^{61}$Ni chemical shift of -1649 ppm, far outside the observed range.

In summary, there is no evidence that the added bulky phosphine could react with **2** to an extent that would alter the expected $^{61}$Ni chemical shift significantly.

What is, then, the reason for the apparent discrepancy between theory and experiment concerning $\delta(^{61}\text{Ni})$ of **2**? An answer to this question can be found taking the line widths of the NMR signals into account. As with many other transition-metal nuclei, quadrupolar line broadening can be a serious obstacle for $^{61}$Ni NMR, because signals for large complexes of low symmetry can be undetectably broad. When relaxation is dominated by the quadrupolar mechanism, the line width $\Delta\nu_{1/2}$ should be proportional to:[45]

$$\Delta\nu_{1/2}\ \propto\ q_{zz}^2(1 + (\eta^2)/3)\tau_c \qquad\qquad (2),$$

that is, it should depend on $q_{zz}$, i.e. the largest component of the electric field gradient (EFG), on the asymmetry parameter $\eta$ defined as $(q_{xx}-q_{yy})/q_{zz}$, and on the molecular correlation time $\tau_c$, which measures the orientational mobility of a molecule and usually increases with molecular size. The

factor $(1 + (\eta^2)/3)$ in eq. 2 can only assume values between 1 and $1\frac{1}{3}$ and is therefore not expected to govern trends covering orders of magnitude. In some instances, e.g. for $^{99}$Tc, computed EFGs have been used successfully to rationalise trends in observed line widths.[46] For consistency with the chemical-shift calculations discussed above, the EFG computations employed the B3LYP functional, affording the results summarised in Table 3.

<Table 3>

The smallest EFG in this set is found for **6** with its near-tetrahedral placement of the four olefin moieties about the metal (for the truly tetrahedral complexes **4** and **9** - **11** the EFG is zero by symmetry). $D_3$-symmetric **1** and its $C_3$-symmetry adducts **7** and **8** are also characterised by fairly small EFGs (around ca. 0.2 a.u., Table 3). In contrast, a much larger $q_{zz}$ value, larger by almost an order of magnitude, is predicted for **2**. Because $q_{zz}$ enters the expression in eq. (2) in form of its square, the line width to be expected for **2** should be nearly eighty times as wide as that of **1**, all other conditions being equal (see $q_{zz}^2$(rel) values in parentheses in Table 3). A substantial EFG, albeit smaller than that of **2**, is also found for the bis(ethylene) complex **5**. In this case, it is probably the smaller size of the complex and, hence, the shorter correlation time $\tau_c$ that makes the $^{61}$Ni resonance recordable.

From the computed EFGs and the observed line width of the $^{61}$Ni resonance of **1**, 3.9 kHz (see section 3.2), the signal for **2** should be more than 0.3 MHz broad, clearly too wide to be detected. It thus appears likely that the resonance at $\delta(^{61}$Ni$) \approx 20$ ppm ascribed to **2** actually originates from traces of its precursor **1** that are still present in the sample (as evidenced, e.g., by the $^{13}$C NMR spectra). The difference between this chemical shift and the one of a solution of pure **1**, $\delta(^{61}$Ni$) = 75$ ppm under the same conditions (section 3.2), may be ascribed to variations in concentration and composition of the two samples. This leads to the somewhat sobering conclusion that the $^{61}$Ni nucleus in **2** is, for all practical purposes, essentially NMR-silent, and that the difference between $\delta(^{61}$Ni$)$ of **1** and **2** predicted by DFT still awaits its experimental confirmation. From the performance study in section 3.1, however, there is little doubt that this computational prediction is reliable, at least qualitatively.

## 4 Conclusions

According to a systematic performance study of representative DFT methods for the computation of $^{61}$Ni chemical shifts, hybrid functionals such as the popular B3LYP combination are superior to

BPW91, a pure GGA functional, which clearly underestimates substituent effects on the $\delta(^{61}Ni)$ values. Because the magnetic shielding constant of $Ni(CO)_4$, the standard for $^{61}Ni$ NMR, shows an unusually strong sensitivity toward the particular functional, an indirect way of referencing the computed relative $^{61}Ni$ chemical shifts is recommended. Using this protocol, experimental $\delta(^{61}Ni)$ values can be reproduced, on average, with an accuracy of ca. 70 ppm.

On going from the all-*trans* cyclododecatriene complex **1** to the all-*cis* isomer **2**, models to study the alleged ring-current effects in the parent ethylene complex **3**, the $^{61}Ni$ nucleus is predicted to be shielded by nearly 700 ppm. Attempts to confirm this result experimentally were thwarted by the apparent failure to record the $^{61}Ni$ NMR signal of **2**. A signal initially ascribed to this species is most likely due to traces of **1** that are still present along with **2**. Key DFT results supporting this interpretation are the computed electric field gradients at the metal, which increase sharply on going from **1** to **2**. Based on these data and the expected quadrupolar relaxation mechanism, an undetectably broad $^{61}Ni$ NMR line is predicted for **2**.

Thus, DFT-computed $^{61}Ni$ chemical shifts and EFGs constitute a valuable complement to $^{61}Ni$ NMR spectroscopy, as they allow for a consistent interpretation of the experimental results. The present study has shown once more how quickly the limits of $^{61}Ni$ NMR experiments are reached and how one can safely resort to DFT computations in such cases.

**References**

1 See: G. Wilke, *Angew. Chem. Int. Ed.,* 1988, **27**, 185-206, and the extensive bibliography therein.

2. C. Elschenbroich, *Organometallics*, 3rd Ed., Wiley-VCH, Weinheim, 2006.

3 D. J. Brauer and C. Krüger, *J. Organomet. Chem.* 1972, **44**, 397-402.

4 E. S. Chernyshova, R. Goddard and K. R. Pörschke, *Organometallics*, 2007, **26**, 4872-4880.

5 K. Fischer, K. Jonas, G. Wilke, *Angew. Chem. Int. Ed.,* 1973, **12**, 565-566.

6 R. Herges and A. Papafilippopoulos, *Angew. Chem. Int. Ed*., 2001, **40**, 4671-4674.

7 See for instance: (a) P. v. R. Schleyer, C. Maerker, A. Dransfeld, H. Jiao and N. J. R. v. E. Hommes, *J. Am. Chem. Soc.,* 1996, **118**, 6317-6318; (b) P. Lazzeretti, *Prog. NMR Spectrosc.*, 2000, **36**, 1-88.

8 This is because the secondary magnetic field induced by a classical ring current is just superimposed onto the local magnetic field at the position of a probe nucleus. For the equivalence of ring-current effects on $^{13}$C and $^1$H chemical shifts of annulenes see for instance: R. du Vernet and V. Boekelheide, *Proc. Nat. Acad. Sci. USA*, 1974, **71**, 2961-2964.

9 (a) M. Bühl and A. Hirsch, *Chem. Rev.*, 2001, **101**, 1153-1184; (b) T. Sternfeld, M. Saunders, R. J. Cross, and M. Rabinovitz, *Angew. Chem. Int. Ed.* 2003, **42**, 3136-3139.

10 (a) P. S. Pregosin (Ed.), *Transition Metal Nuclear Magnetic Resonance*, Elsevier: Amsterdam, 1991; (b) W. von Philipsborn, *Chem. Soc. Rev.,* 1999, **28**, 95-106.

11 E.g.: a) A. G. Avent, F. Geoffrey, N. Cloke, J. P. Day, AE. A. Seddon, K. R. Seddon and S. M. Smedley, *J. Organomet. Chem.*, 1988, **341**, 535-541; b) R. Benn and A. Rufinska, *Magn. Reson. Chem.*, 1988, **26**, 895-902; c) K. D. Behringer and J. Blümel, *Magn. Reson. Chem.*, 1995, **33**, 729-733.

12 Review: R. Benn and A. Rufinska, *Angew. Chem. Int. Ed.* 1986, **25**, 861-881.

13 D. Peters, PhD thesis, University of Kiel (Germany), 2006.

14 See M. Bühl, *Ann. Rep. NMR Spectrosc.*, 2008, **64**, 77-126 and the extensive bibliography therein.

15 See for instance: (a) M. Bühl M, *Chem. Phys. Lett.*, 1997, **267**, 251-257; (b) M. Bühl and F. A. Hamprecht, *J. Comput. Chem.,* 1998, **119**, 113-122; (c) M. Bühl, S. Gaemers and C. J. Elsevier, *Chem. Eur. J.*, 2000, **6,** 3272-3280; (d) M. Bühl, *Theor. Chem. Acct.*, 2002, **107**, 336-342; (e) M. Bühl and F. T. Mauschick, *Magn. Reson. Chem.*, 2004, **42**, 737-744.

16 A. D. Becke, *Phys. Rev. A,* 1988, **38**, 3098-3100.

17 (a) J. P. Perdew, *Phys. Rev. B,* 1986, **33**, 8822-8824; (b) J. P. Perdew, *Phys. Rev. B,* 1986, **34**, 7406.

18 (a) W. J. Hehre, R. Ditchfield and J. A. Pople, *J. Chem. Phys.*, 1972, **56**, 2257-2261; (b) P. C. Hariharan and J. A. Pople, *Theor. Chim. Acta.*, 1973, **28**, 213-222.

19 J. R. Cheeseman, G. W. Trucks, T. A. Keith and M. J. Frisch, *J. Chem. Phys.*, 1996, **104**, 5497-5509.

20 (a) J. P. Perdew, in: P. Ziesche and H. Eischrig (Eds.), *Electronic Structure of Solids*, Akademie Verlag, Berlin, 1991; (b) J. P. Perdew and Y. Wang, *Phys. Rev. B,* 1992, **45**, 13244-13249.

21  A. D. Becke, *J. Chem. Phys.*, 1993, **98**, 5648-5652.

22 C. Lee, W. Yang and R. G. Parr, *Phys. Rev. B,* 1988, **37**, 785-789.

23 Defined as $0.5 * E_X^{HF} + 0.5 * E_X^{LSDA} + E_C^{LYP}$; for the original formulation of the "half-and-half" hybrid functional see: A. D. Becke, *J. Chem. Phys.*, 1993, **98**, 1372-1377.

24 W. Kutzelnigg, U. Fleischer and M. Schindler, In: *NMR Basic Principles and Progress Vol. 23*, Springer-Verlag: Berlin, 1990, p. 165.

25 6-31G(d) basis for Ni: V. A. Rassolov, M. A. Ratner, J. A. Pople, P. C. Redfern and L. A. Curtiss, *J. Comput. Chem.*, 2001, **22**, 976-984.

26 Frisch, M. J.; Trucks, G. W.; Schlegel, H. B.; Scuseria, G. E.; Robb, M. A.; Cheeseman, J. R.; Zakrzewski, V. G.; Montgomery, J. A.; Stratman, R. E.; Burant, J. C.; Dapprich, S.; Millam, J. M.; Daniels, A. D.; Kudin, K. N.; Strain, M. C.; Farkas, O.; Tomasi, J.; Barone, V.; Cossi, M.; Cammi, R.; Mennucci, B.; Pomelli, C.; Adamo, C.; Clifford, S.; Ochterski, J.; Petersson, G. A.; Ayala, P. Y.; Cui, Q.; Morokuma, K.; Malick, D. K.; Rabuck, A. D.; Raghavachari, K.; Foresman, J. B.; Cioslowski, J.; Ortiz, J. V.; Baboul, A. G.; Stefanov, B. B.; Liu, C.; Liashenko, A.; Piskorz, P.; Komaromi, I.; Gomperts, R.; Martin, R. L.; Fox, D. J.; Keith, T.; Al-Laham, M. A.; Peng, C. Y.; Nanayakkara, A.; Gonzalez, C.; Challacombe, M.; Gill, P. M. W.; Johnson, B. G.; Chen, W.; Wong, M. W.; Andres, J. L.; Gonzales, C.; Head-Gordon, M.; Replogle, E. S.; Pople, J. A., Gaussian, Inc., Pittsburgh PA, 1998.

27 B. Bogdanovic, M. Kröner, and G. Wilke, *Liebigs Ann. Chem.* 1966, **699**, 1-23.

28 K. Jonas, Über die Wechselwirkung von Phosphinen bzw. Phosphiten und Ringolefinen mit Nickel(0), Ph.D. Thesis, Ruhr-Universität Bochum (Germany), 1968.

29 See for instance: (a) E. G. Hoffmann, P. W. Jolly. A. Kusters, R. Mynott and G. Wilke, *Z. Naturforsch. B*, 1976, **31**, 1712-1713. (b) P. W. Jolly and R. Mynott, *Adv. Organomet. Chem.*, 1981, **19**, 257-304. (c) K. R. Pörschke, K. Jonas, G. Wilke, R. Benn, R. Mynott, R. Goddard and K. Krüger, *Chem. Ber.*, 1985, **118**, 275-297.

30 K. Jonas, P. Heimbach, and G. Wilke, *Angew. Chem. Int. Ed. Engl.* 1968, **7**, 949-950.

31 S. D. Ittel, H. Berke, H. Dietrich, J. Lambrecht, P. Härter, J. Opitz and W. Springer, *Inorg. Synth.* 1977, **17**, 117-124

32 L. Hedberg, T. Iijima and K. Hedberg, *J. Chem. Phys.* 1979, **70**, 3224-3229.

33 Almenningen, A.; Andersen, B.; Astrup, E. E. *Acta Chem. Scand.* 1970, **24**, 1579-1584

34 (Menthyl)dimethylphosphane complex: G. Wilke, *Angew. Chem. Int. Ed.*, 1988, **27**, 185-206.

35 P. Macchi, D. M. Proserpio, and A. Sironi, *J. Am. Chem. Soc.* 1998, **120**, 1447-1455.

36 Monodentate $t$Bu$_2$PCH$_2$P$t$Bu$_2$ ligand: T. Nickel, R. Goddard, Carl Krüger and K. R. Pörschke, *Angew. Chem. Int. Ed.*, 1994, **33**, 879-882.

37 See for instance: W. Koch and M. C. Holthausen, *A Chemist's Guide to Density Functional Theory*, Wiley-VCH: Weinheim, 2000, and the extensive bibliography therein.

38 Specifically the TPSS-hybrid, see: M. Bühl and H. Kabrede, *J. Chem. Theory Comput.*, 2006, **2**, 1282-1290.

39 M. Bühl, *Magn. Reson. Chem.*, 2006, **44**, 661-668.

40 See S. Grigoleit and M. Bühl, *Chem. Eur. J.*, 2004, **10**, 5541-5552 and references cited therein.

[41] Electronic factors disfavour the formation of **2**·L complexes with tetrahedral coordination about the metal, to the extent that not even a PMe$_3$ adduct can be isolated, cf. ref. 4.

42 *anti* orientation between the single (P)C-H bond and the P-M axis was assumed throughout, as this has been found to be the most stable form in the corresponding trialkylphosphane selenide, see: C. G. Hrib, F. Ruthe, E. Seppälä, M. Bätcher, C. Druckenbrodt, C. Wismach, P. G. Jones, W.-W du Mont, V. Lippolis, F. A. Devillanova and M. Bühl, *Eur. J. Inorg. Chem.*, 2006, 88-100.

43 With a chelating bis-phosphine, a $\eta^2$-complex similar to **13b** can be isolated (cf. compound **7b** in ref. 4); arguably the repulsion of the two bulky monodentate phosphines, evidenced by the large P-Ni-P bite angle of 127.5°, contributes to the destabilisation of **13b**.

44 No (tris)phosphine complex can be located, as an attempted optimisation of Ni{P(*t*Bu)$_2$(*i*Pr)}$_3$ results in dissociation of one phosphine.

45 A. Abragam (Ed.), *The Principles of Nuclear Magnetism*, Oxford University Press, Oxford, 1961, Chapter 9, p. 314.

46 See M. Bühl andV. Golubnychiy, *Magn. Reson. Chem.*, 2008, **46**, S36-S44, and further examples cited therein.

**Table 1**. Optimised geometrical parameters for Ni complexes **1** - **11** (bond distances and angles in Å and degrees, respectively), together with experimental values, where available.

| Molecule | symmetry | parameter | BP86/AE1 | Expt. | Ref. |
|---|---|---|---|---|---|
| Ni(t,t,t-cdt) (**1**) | $D_3$ | Ni-C1 | 2.047 | 2.024(2) | 3 |
| | | C1=C2 | 1.403 | 1.372(5) | |
| | | X1-Ni-C1-X2[b] | 58.2 | 59.0 | |
| Ni(c,c,c-cdt) (**2**) | $C_3$ | Ni-C1 | 2.043 | 2.119(6)[c] | 4 |
| | | Ni-C2 | 2.070 | 2.298(12)[c] | |
| | | C=C | 1.405 | 1.440(12)[c] | |
| | | X1-Ni-C1-X2[b] | 85.9 | | |
| Ni(C$_2$H$_4$)$_3$ (**3a**) | $D_{3h}$ | Ni-C | 2.053 | | |
| | | C=C | 1.400 | | |
| Ni(CO)$_4$ (**4**) | $T_d$ | Ni-C | 1.829 | 1.825(2) | 32 |
| Ni(C$_2$H$_4$)$_2$(PMe$_3$) (**5**) | $C_3$ | Ni-C1 | 2.008 | 2.000(2) | 36 |
| | | Ni-C2 | 2.011 | 2.015(2) | |
| | | Ni-P | 2.177 | 2.238(1)[d] | |
| | | C1=C2 | 1.412 | 1.383 | |
| Ni(cod)$_2$ (**6**) | $C_2$ | Ni-C1 | 2.121 | 2.124(9) | 35 |
| | | Ni-C2 | 2.140 | 2.124(9) | |
| | | C1=C2 | 1.401 | 1.391(2) | |
| Ni(t,t,t-cdt)(CO) (**7**) | $C_3$ | Ni-C1 | 2.143 | | |
| | | Ni-C2 | 2.176 | | |
| | | Ni-C(O) | 1.789 | | |
| | | C1=C2 | 1.392 | | |
| Ni(t,t,t-cdt)(PMe$_3$) (**8**) | $C_3$ | Ni-C1 | 2.103 | 2.091 | 34 |
| | | Ni-C2 | 2.146 | 2.128 | |
| | | Ni-P | 2.221 | 2.238[d] | |
| | | C1=C2 | 1.400 | 1.372(5) | |
| Ni(PF$_3$)$_4$ (**9**) | $T$ | Ni-P | 2.107 | 2.099(3) | 33 |
| Ni(PMe$_3$)$_4$ (**10**) | $T$ | Ni-P | 2.180 | | |
| Ni(PCl$_3$)$_4$ (**11**) | $T_d$ | Ni-P | 2.154 | | |

[a] cod = 1,5-cyclooctadiene, c,c,c-cdt and t,t,t-cdt denote all-cis- and all-trans-1,5,9-cyclododeca-triene, respectively. [b] X1 is a point on the threefold axis, X2 the midpoint of the C=C double bond. [c] CH=CH and CH$_2$-CH$_2$ bonds disordered. [d] Bulkier phosphine used experimentally (see references).

**Table 2**. Theoretical $^{61}$Ni chemical shifts, computed using BP86/ geometries, GIAO-DFT methods, basis II', together with experimental data.[a]

| Molecule | BPW91 | B3LYP | BHandHLYP | Expt. |
|---|---|---|---|---|
| Ni(t,t,t-cdt) (**1**) | 181 | 201 | 202 | 206 |
| Ni(CO)$_4$ (**4**) | 61 | 284 | 548 | 0 |
| Ni(C$_2$H$_4$)$_2$(PMe$_3$) (**5**) | -865 | -937 | -973 | -866 |
| Ni(cod)$_2$ (**6**) | 709 | 802 | 1015 | 937 |
| Ni(t,t,t-cdt)(CO) (**7**) | 657 | 760 | 832 | 747 |
| Ni(t,t,t-cdt)(PMe$_3$) (**8**) | 757 | 854 | 969 | 922 |
| Ni(PF$_3$)$_4$ (**9**) | -708 | -738 | -824 | -929 |
| Ni(PMe$_3$)$_4$ (**10**) | 15 | 23 | 0 | 40 |
| Ni(PCl$_3$)$_4$ (**11**) | 312 | 245 | 150 | 267 |
| | | | | |
| slope [b] | 0.85 | 0.93 | 1.04 | |
| MAD [c] | 101 | 65 | 73 | |

[a] Magnetic shielding constant of the standard evaluated via $\sigma_{calc}$ vs. $\delta_{expt}$ correlations, see text; experimental data from reference 11.

[b] Slope of the $\delta_{calc}$ vs. $\delta_{expt}$ linear regression line (excluding **4**).

[c] Mean absolute deviations between experimental and computed chemical shifts (excluding **4**).

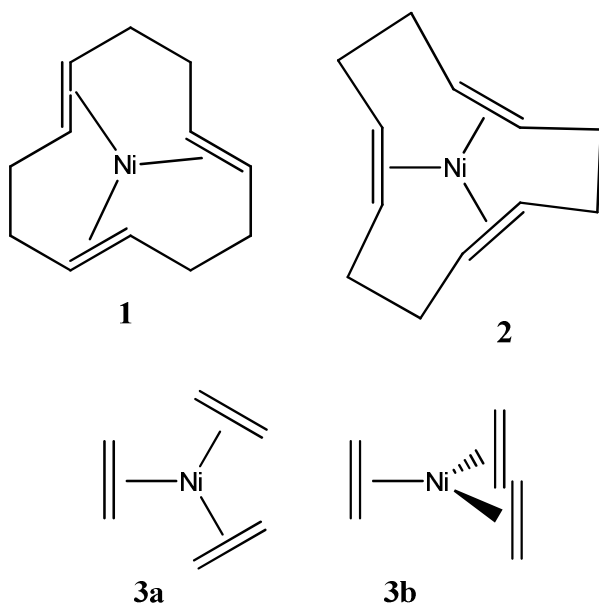**Table 3**. Computed EFGs[a] of the Ni nucleus in Ni complexes. In parentheses: squared values relative to **1**.

| Molecule | $q_{zz}$ | $q_{zz}^2$(rel)[b] |
|---|---|---|
| Ni(t,t,t-cdt) (**1**) | 0.153 | (1) |
| Ni(c,c,c-cdt) (**2**) | 1.358 | (79) |
| Ni(C$_2$H$_4$)$_2$(PMe$_3$) (**5**) | 0.963[c] | (40) |
| Ni(cod)$_2$ (**6**) | 0.066[d] | (0.2) |
| Ni(t,t,t-cdt)(CO) (**7**) | 0.221 | (2) |
| Ni(t,t,t-cdt)(PMe$_3$) (**8**) | 0.276 | (3) |

[a] Largest components $q_{zz}$ of the EFG tensor (in a.u.), B3LYP/II'//BP86/AE1 level; $\eta$ = 0 except where otherwise noted.
[b] Relative values with respect to **1**.
[c] $\eta = 0.20$
[d] $\eta = 0.87$

**1**

**2**

**3a**

**3b**

**Scheme 1**



**4** ($T_d$)

**5** ($C_s$)

**6** ($C_2$)

**7** X=CO ($C_3$)
**8** X=PMe$_3$ ($C_3$)

**9** X=F ($T_d$)
**10** X=Me ($T$)
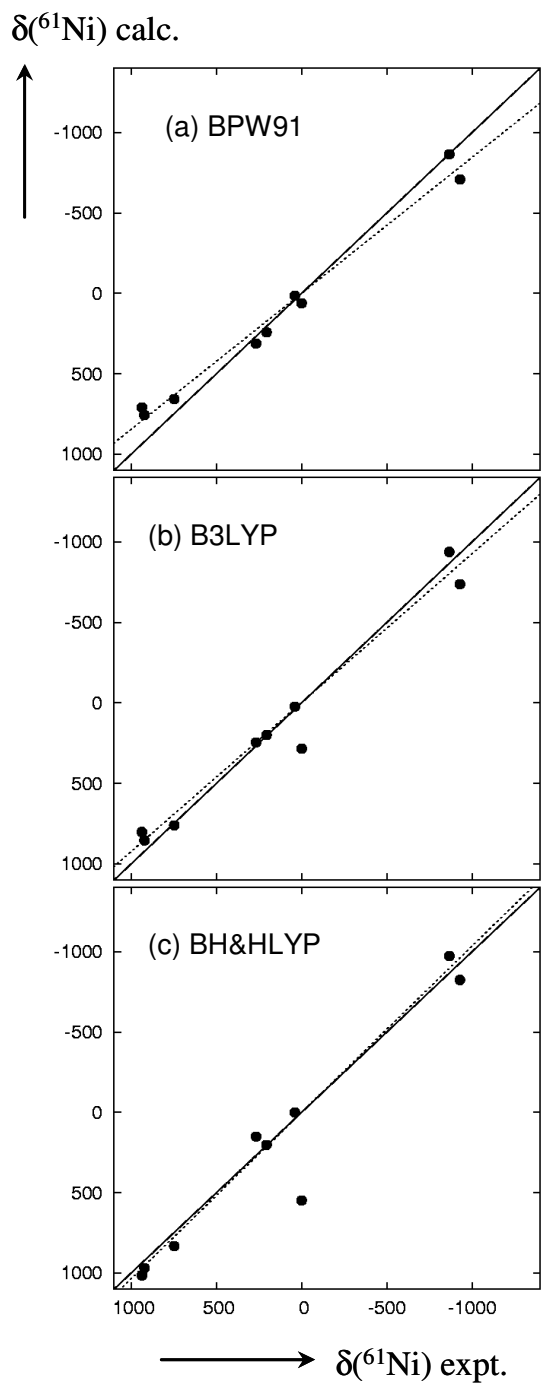**11** X=Cl ($T_d$)

**Scheme 2**

**Figures**



**Figure 1**: Plot of GIAO-DFT computed vs. experimental $^{61}$Ni chemical shifts, including linear regression lines (dashed, excluding the data point for **4** at $\delta_{expt}$ =0) and the ideal line with the slope 1 (solid).
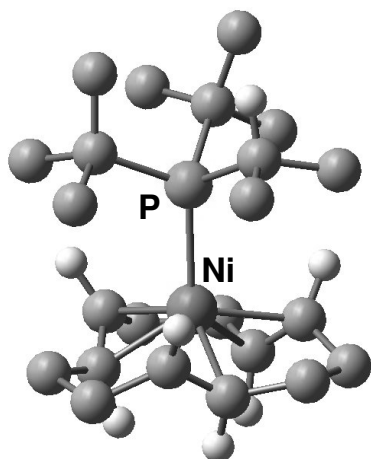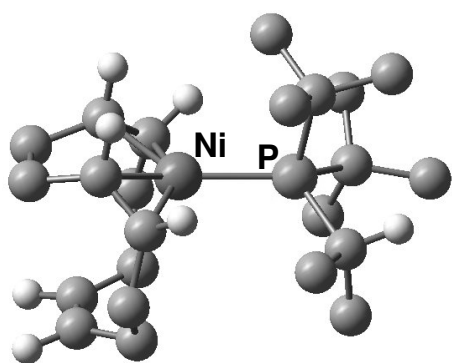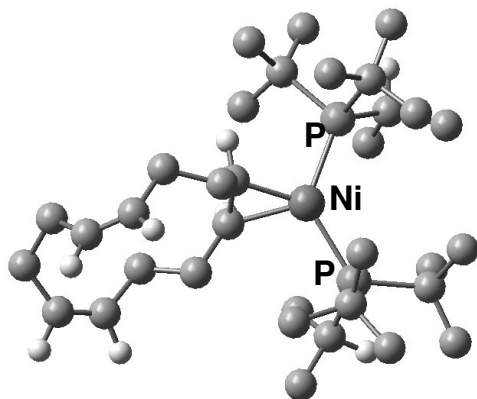
**12** (δ = 1233)

**13a** (δ = −55)

**13b** (δ = 415)

**Figure 2**: Optimised Ni(cdt)-P($t$Bu)$_2$($i$Pr) adducts (methyl and methylene H atoms omitted for clarity), together with GIAO-B3LYP computed $^{61}$Ni chemical shifts

**Table of Contents Entry**

**Substituent Effects on $^{61}$Ni NMR Chemical Shifts.**

**Michael Bühl, Dietmund Peters and Rainer Herges**

DFT methods are assessed in their capability to reproduce $^{61}$Ni chemical shifts of a number of inorganic and organometallic Ni complexes. The computations predict a highly shielded metal nucleus in the (all-*cis*-cyclododecatriene)-nickel(0) complex, but also an extremely broad $^{61}$Ni NMR resonance, thereby rationalizing the apparent failure to detect the latter experimentally.